Semiconductor Physics, Quantum Electronics & Optoelectronics, 2024. V. 27, No 4. P. 478-488.

Sensors

Spectral SPR effect in thin films of high-conductive metals and features of SPR-biosensors implementation in chromatic mode

O.L. Kukla, Yu.M. Shirshov, A.I. Biletskiy, O.N. Fedchenko

V. Lashkaryov Institute of Semiconductor Physics, NAS of Ukraine
41, prospect Nauky, 03028 Kyiv, Ukraine,
Corresponding author e-mail: alex.le.kukla@gmail.com

Abstract. In this paper, we have evaluated the application of various types of highly conductive metals for implementing the effect of spectral surface plasmon resonance (SPR) within a visible spectrum range to achieve more efficient and productive registration of biomolecules in a liquid medium using tricolor RGB cameras. Thin films of gold, silver, copper, and aluminum, as well as a bimetallic coating of silver with a gold superlayer on a glass substrate, are considered. Detailed calculations of the spectral characteristics of reflection at SPR excitation in the Kretschmann geometry are performed, particularly when a thin dielectric film is formed on the metal surface that imitates a layer of biomolecules. For each of the specified metals, the width of the region of implementation of the full-fledged SPR effect in the visible range of the spectrum is determined, and the sensitivity of the optical response to the influence of an external dielectric layer is assessed.

Keywords: spectral SPR effect, chromatic mode, high-conductive metals, reflection spectra, R, G, B components, visible wavelengths range.

https://doi.org/10.15407/spqeo27.04.478
PACS 73.20.Mf, 78.40.-q, 87.85.fk

Manuscript received 03.09.24; revised version received 04.10.24; accepted for publication 13.11.24; published online 06.12.24.

1. Introduction

The method of surface plasmon-polariton resonance is widespread for recording the interactions of biomolecules on the surface of a thin metal film and is widely used in practical applications [1–4]. Today, many devices for biomolecules registering in solution have been created based on this method [5–9]. However, there is still a need to increase the productivity of these devices by creating multichannel analyzers capable of detecting the presence of dozens of biomolecule types in the analyzed mixture. The need for direct recording of the unfolding and hybridization of DNA segments during polymerase reactions remains very relevant [10, 11].

Thin gold films with developed surface chemistry methods for the controlled binding of specific ligands are usually used for SPR sensor applications. However, the surface plasmon resonance (SPR) effect in gold films is realized within the red and infrared spectral regions, and its registration requires the use of spectrometers. This significantly limits design options. In the case of silver films, the SPR effect can be realized within a shorter-wavelength region of the spectrum. Moreover, to implement the SPR sensor in the chromatic mode, it is possible to use other metals with high electrical conductivity – copper and aluminum.

Therefore, it is necessary to analyze the suitability of all the above-mentioned highly conductive metals for the implementation of a chromatic SPR sensor. The question of choosing the type of metal for registering the influence of medium refraction on the SPR effect was raised more than 30 years ago [12], but it did concern the possibility of chromatic registration at that time. At the same time, modern optical technology of the visible range (CCD and web cameras) allows easy and quick capture of video information, relying on the registration of the main components of white light (R, G, and B). In the mentioned work [12], the concept of sensitivity of the SPR effect in the Kretschmann geometry to the appearance of a thin dielectric film on the surface of metals, namely: Al, Cd, Cu, In, Au, and Ag, was introduced for the first time. The authors concluded that silver possesses optical constants providing the highest detection sensitivity. Much later, in work [13], a method to protect the silver surface from chemical influences with a thin polymer film was proposed, and in [14], the use of a bimetallic structure in the form of a thinner gold film on the surface of a thicker silver film was proposed and optimized (a similar conclusion was made in the review [3]).

The practical implementation of chromatic registration can be carried out in different ways. We will mention only some of the known technical solutions. In [15],

a sapphire semi-cylinder was used onto the axis on which a converging white beam was focused. The reflected beam was collimated by a cylindrical lens and passed through a diffraction grating, which allows for recording of the spectrum of the refractive index of a water/glycerol solution within the red and near IR ranges (580…710 nm). Later, in [16], the chromatic registration of the SPR minimum was implemented using the light pipe method (an intermediate option between a prism and a planar waveguide) with a gold film. In work [17], a detailed comparison of the spectral and angular options for SPR control was carried out and it was shown that in terms of sensitivity, the use of a goniometer (with an accuracy of 0.001 deg.) is equivalent to the chromatic approach with an accuracy of 0.6 nm.

Recently, significant attention has been paid to the search for new materials suitable for SPR registration [18–32]. This interest arises from the growing demand for biosensing technologies in the fields of medical diagnostics, environmental monitoring, and food safety. However, researchers are not only exploring novel materials but, also, working to replace traditional dispersive elements like prisms or diffraction gratings with tricolor cameras, enabling the development of multichannel bioanalyzers for simultaneous analysis of multiple analytes. Thus, studies [33, 34] substantiate the use of smartphones in medical analyzers, showcasing their accessibility and potential for rapid diagnostics. Additionally, the work [35] demonstrates the application of three RGB LEDs to create an express analyzer for detecting sugar and albumin in urine. The authors of [36] highlight the usefulness of color shades in the RGB space for a detailed analysis of the SPR reflection spectrum, offering a more efficient alternative to detailed spectral data.

The main goal of this work is to evaluate the feasibility of using various types of highly conductive metals to implement the SPR spectral effect within the visible range of the spectrum to achieve more sensitive registration of biomolecules.

2. Theoretical background

The spectral range of occurrence of the SPR effect in thin metal films is determined by the optical parameters of the metal and the dielectric. Thus, the condition for the existence of plasmon-polariton resonance at the metal-dielectric interface is the accordance of the relation $\varepsilon_m < -\varepsilon_d$, where ε_m is the real part of the permittivity of the metal (it is negative), ε_d is the permittivity of the dielectric. Recall that the optical constants of metal n, k are related to the complex permittivity $\varepsilon' + i\varepsilon''$ as follows: $(n + ik)^2 = \varepsilon' + i\varepsilon''$. In the case of the Kretschmann geometry, the adjustment of the X-component of the photon wave vector is carried out by varying the angle of incidence at a given wavelength, focusing on a type of metal. The spectral dependences of optical parameters n, k for thin films of gold, silver, copper, and aluminum are shown in Fig. 1a. The values of these parameters within the visible spectral range were obtained from a publicly available reference site [37], and in general, they correspond to the literature data [38, 39]. Based on preliminary estimates of the extinction coefficients (they determine the attenuation of a light wave in metal), the film thicknesses necessary for implementing SPR in them were selected within the ranges: 50…55 nm for gold, 35…40 nm for silver, 30…35 nm for copper, and 20…25 nm for aluminum. As can be seen, the highest value of the k parameter is observed for aluminum, and it is significantly smaller for silver; copper and gold show close and slightly smaller values. At the same time, the refractive index has the lowest value for silver within the entire wavelength range. Gold and copper show a decreasing dependence with increasing wavelength, and aluminum – an increasing one. Fig. 1b shows the corresponding values of the real part of a dielectric function $\varepsilon_m = n^2 - k^2$ of the specified metals compared with the value of the dielectric constant of water ($\varepsilon_d = 1.769$, $n_d = 1.33$). As we can see, the above condition for the existence of SPR for gold films is realized only within the long-wave region at wavelengths $\lambda > 500$ nm. For other considering metals Ag, Cu, and Al, such restrictions are not observed. Therefore, it can be assumed that for some of them, it will be possible to implement a chromatic SPR biosensor within the entire visible range of wavelengths.

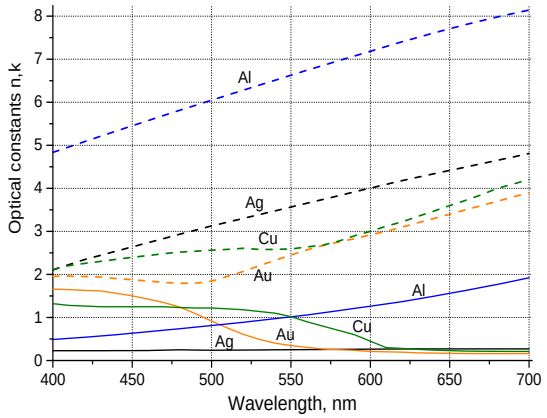

Fig. 1a. The spectral dependences of the refractive index n (solid curves) and extinction k (dashed curves) for films of highly conductive metals Au, Ag, Cu, and Al.

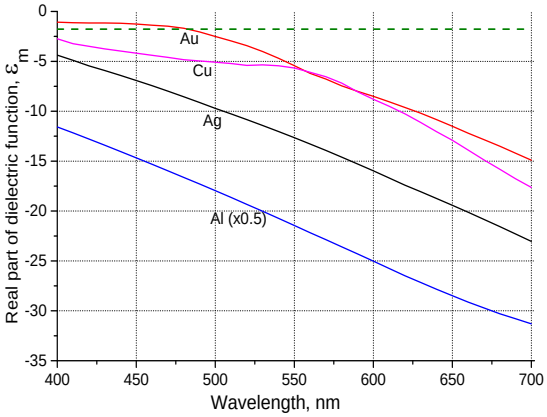

Fig. 1b. The spectral dependences of the real part ε_m of the permittivity of specified metals. The dashed line indicates the value ε_d for water.

Let us calculate the spectral and angular dependences of the reflection coefficient R on the excitation of SPR in the Kretschmann geometry for a semi-cylindrical glass prism with a refractive index of 1.61 in films of all specified types of metals to determine the width of the region of implementation of the full-fledged SPR effect within the range of visible wavelengths. The estimation of the effect of an external thin dielectric layer (a 5…10 nm thick film with a refractive index of 1.48 (ε_d =2.19), close to the refraction value of oligonucleotide layers) deposited on the metal surface is also important. The calculations were performed using the freely available WinSpall 3.02 program for modeling SPR curves [40], created based on the Fresnel formalism. The spectral dependences of the n, k values of metals are taken from the data in Fig. 1a. For certainty, the following film thicknesses were taken for the calculations of reflectance spectra: 50 nm for gold, 40 nm for silver, 35 nm for copper, and 20 nm for aluminum.

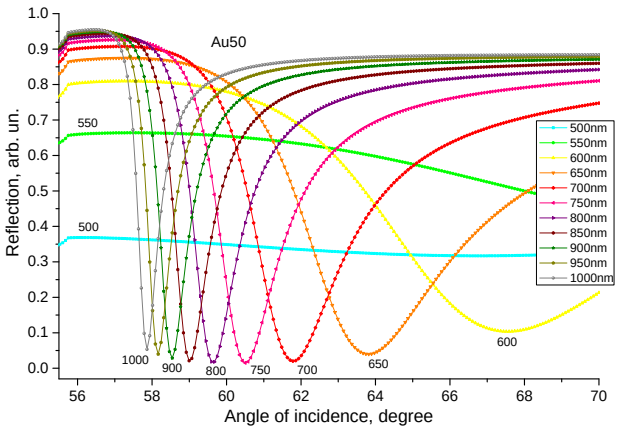

Fig. 2a. The evolution of the reflection coefficient with the excitation of SPR in a 50 nm thick gold film in contact with water within the red spectrum range 500…1000 nm (wavelength values with the step of 50 nm are indicated on the curves). For interpretation of the colors in the figure(s), the reader is referred to the web version of this article.

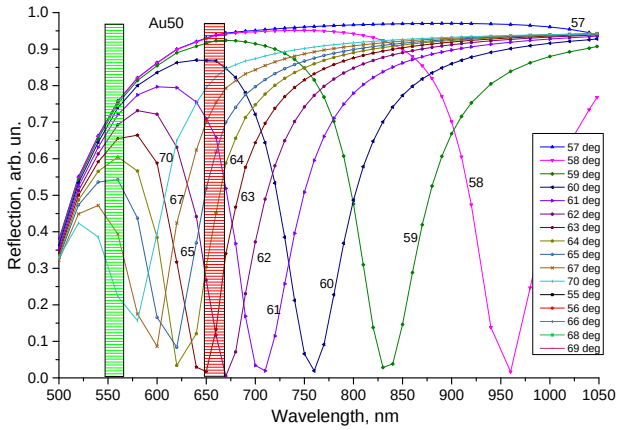

Fig. 2b. The family of spectral dependences of the reflectivity of a 50 nm thick gold film at different fixed angles of light incidence (the angle values are shown on the curves). The vertical colored bars indicate the position of spectral components R (at 660 nm) and G (at 560 nm).

Gold

Fig. 2a shows the calculated SPR reflection spectra $R(\theta)$ in the scale of light incidence angles for a gold film within the range 500…1000 nm. The longest-wavelength curve (on the left) corresponds to 1000 nm, the rest were obtained with a wavelength value shift of 50 nm toward a decrease. One can observe that the narrowest resonance curve belongs to the longest IR wave. The minimum of the curve greatly expands and practically disappears with decreasing the wavelength to 500 nm.

Fig. 2b shows similar dependences of internal light reflection from the glass-gold-water interface $R(\lambda)$, calculated on the wavelength scale at fixed angles of light incidence. It is seen that at angles 61…63 degrees there is a full-fledged deep minimum of internal reflection of light, which falls on the red component of white light. However, starting from angles of incidence of 65 to 66 degrees, the minimum becomes increasingly shallow, although it still partially covers the green part of the spectrum. In fact, this weakened green band is the short-wave limit of the possibility of implementing of SPR on gold. Note that the blue region is inaccessible in this case.

Since the main purpose of the SPR sensor is to register biomolecules from a solution on the metal surface, we will simulate this process by creating a thin dielectric layer between metal and liquid. A model calculation of this effect is shown in Fig. 3.

We see that the appearance of a thin film leads to a shift of the curve $R(\theta)$ to the right, so that the reflection signal on the left slope of the curve increases, and on the right slope, it decreases (which is illustrated by pairs of arrows *1-1'*, *2-2'*, and *3-3'*). The magnitude of the shift can be used as a basis for assessing the sensitivity S of the SPR sensor to a change in the thickness of the dielectric layer. In this case, the shift value can be recorded in two ways: 1) by the shift of the SPR minimum angle at a fixed wavelength, S_1, and 2) by the change in the reflection coefficient R at a fixed angle of incidence, S_2.

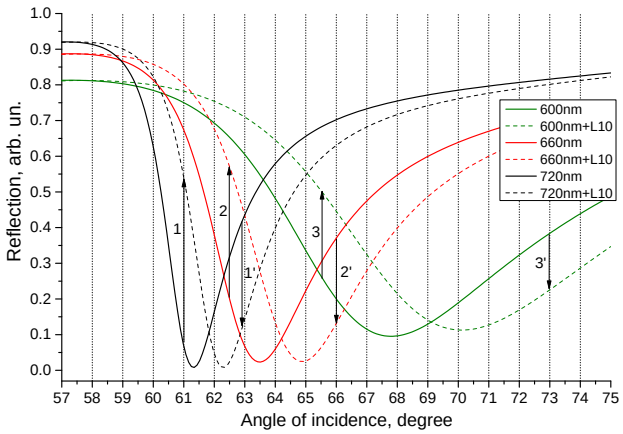

Fig. 3. The response of an internal reflection in a gold film to the appeared 10 nm thick dielectric layer with a refractive index of 1.48 at three incident light wavelengths of 720, 660, and 600 nm. The arrows (*1-1'*), (*2-2'*), and (*3-3'*), respectively, show the change in the reflectivity at selected fixed angles of incidence, as a response to the appearance of the outer film.

Thus, based on the curves in Fig. 3, for wavelengths corresponding to the red and near IR spectral regions relevant for gold, we obtained the following sensitivity ranges: S_1 = 1…2 degrees, S_2 = 0.23…0.46 arb. un.

It should be noted that the opposite signal shift can be successfully used to enhance the response if it is calculated as the difference between signals taken from different sides of the minimum. Moreover, this can be achieved in two ways: either with two fixed wavelengths of one angle of incidence or with two fixed angles of one wavelength. The first way of this response difference was previously used in work [41]. For example, based on Fig. 2b, the optimal wavelengths for this recording principle at an incidence angle of θ = 62° can be λ_1 = 630…650 nm and λ_2 = 700…720 nm, while based on Fig. 3, accordingly, the optimal angles for λ = 720 nm are θ_1 = 60.5…61° and θ_2 = 62.5…63°. Thus, there is a certain reserve for increasing the sensitivity of this method when switching to shorter or longer wavelengths.

Thus, considering the gold films the following can be noted. Gold films used in the chromatic SPR mode can fully operate only within the red and infrared range at wavelengths over 500 nm. However, working in the long-wave range, the inconvenience is caused by the invisibility of IR rays and the need to use synchronous detection. On the other hand, the advantage of using gold is the availability of well-developed methods for its surface modification for biosensorics.

Silver

Fig. 4a shows a family of model SPR reflectance curves $R(\theta)$ for 40 nm thick silver films in contact with water within the visible wavelength range. Unlike gold, a full minimum of SPR reflection is observed here throughout the entire visible range of waves from 700 nm up to 400 nm, allowing the use of this range for RGB registration. The minimum broadens with shortening the wavelength, but it will be shown below that the angular sensitivity to the appearance of a dielectric layer on the silver surface also increases with broadening the minimum.

The spectral reflection curves calculated in the wavelength scale $R(\lambda)$ at fixed angles of light incidence in the case of pure silver are shown in Fig. 4b. One can see that these curves have a U-shaped form with a deep minimum of reflection for all angles within the range 59°…70°. The vertical colored bars indicate the positions of all three spectral components R (at 660 nm), G (at 560 nm), and B (at 460 nm).

As can be seen from Fig. 4b, in the case of pure silver, to enhance the response as the difference of signals at two fixed wavelengths obtained from either side of SPR minimum, responses at two wavelengths can be used, either on the blue and green bands (at angles 67°…68°) or on the green and red bands (at angles 61°…62°). If all three color components are used and an optical scheme with angles of incidence of the white beam at 61 and 67 degrees is chosen, one can expect a doubling of the magnitude of the registered effect.

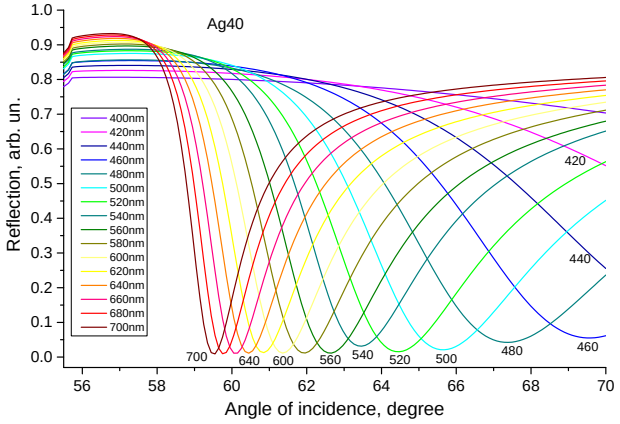

Fig. 4a. The spectral dependences of the reflectance coefficient on the excitation of SPR in a 40 nm thick silver film in contact with water; the initial wavelength of 700 nm is shortened stepwise by 20 nm up to 400 nm.

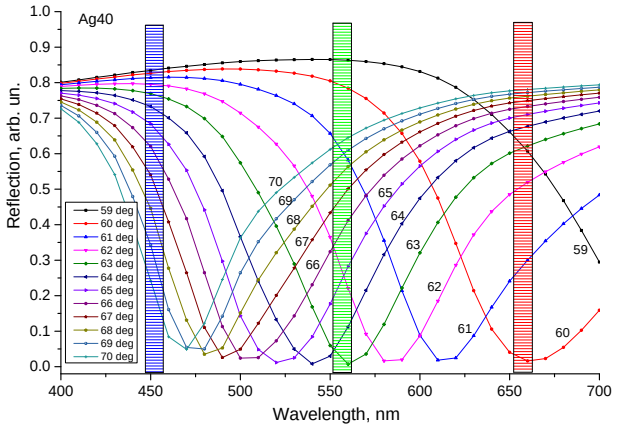

Fig. 4b. The spectral dependences of the internal reflection for a 40 nm thick silver film at different angles of light incidence. The colored bars indicate the positions of spectral components R, G, and B.

Let us evaluate the reaction of the reflection coefficient R to the appearance of a thin dielectric film on the surface of silver. This assessment for three wavelengths corresponding to the R, G, and B components is shown in Fig. 5. As we can see, the obtained sensitivity is quite high. According to the criteria introduced above, the angular shift of the SPR minimum S_1 at a fixed wavelength and the change in the magnitude of the reflection coefficient S_2 at a fixed angle of incidence lies within the following ranges: S_1 = 1…4 degrees, S_2 = 0.36…0.5 arb. un.

A well-known drawback of silver is its chemical reactivity, which necessitates covering the surface of the metal that contacts the aqueous environment. For this purpose, the use of a thin polymer coating on silver that can neutralize its chemical activity can be proposed. In this case, the polymer coating can simultaneously perform as a selective and sensitive layer for the SPR sensor [42]. However, a more traditional approach, in this case, is to apply a sufficiently thin layer of gold onto the silver [14].

Bimetallic layer silver-gold

Let us simulate the application of a thin (5 nm) gold overlayer onto a silver film of 40 nm thick. This bimetallic coating was proposed in [14]. The results of calculating the family of the spectral dependences of reflection in the angular scale at different wavelengths for this case are shown in Fig. 6a.

A comparison of the obtained curves with similar ones for a pure silver film (see Fig. 4a) shows that after applying a thin gold overlayer on silver, the SPR excitation spectrum significantly shortens within the short-wavelength region, shifting from 460 nm (blue region) to 500 nm (beginning of the green region) at the same angles. At the same time, there is a noticeable narrowing of the SPR minimum within this range.

The dashed curves in Fig. 6a show the result of the appearance of thin "adsorption" 5 nm layer with a refractive index of 1.48 on the bimetallic film. As can be seen, the appearance of the thin layer on the surface leads to a characteristic shift of the SPR curve towards larger angles. However, within the green region, there is a narrowing of the minimum of the curve, and with further movement towards the blue region of the spectrum, the excitation of the plasmon-polariton is disrupted precisely due to the appearance of the thin gold overlayer. The reflection curves for the examined bimetallic structure, presented in the wavelength scale at fixed angles (within the range 59°…70°), are shown in Fig. 6b. The vertical red and green bars correspond to the regions of successful registration of the color components R and G. However, the blue region turns out to be inaccessible.

A distinct and quite narrow minimum is observed for angles of 60 to 64° (see Figs 6a, 6b). At an angle of 60°, the minimum is located close to 700 nm, and "adsorption" leads to its shift to 680 nm. Increasing the angle of incidence gradually moves the minimum to the left. However, the response to "adsorption" gradually decreases with increasing the angle of incidence. The

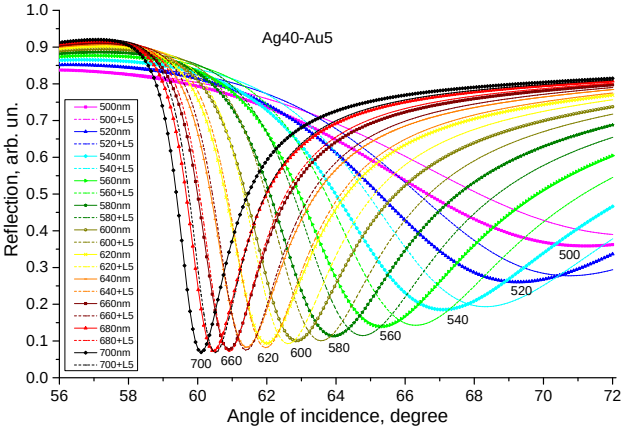

Fig. 6a. The angular dependences of SPR for the bimetallic film Ag40-Au5; wavelength values with the step of 20 nm are indicated on the curves. The dashed curves show the effect of an external 5 nm dielectric film (n = 1.48).

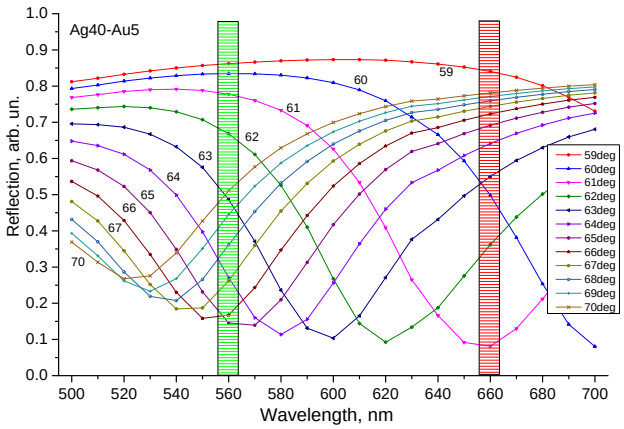

Fig. 6b. The spectral dependences of reflection for the bimetallic structure Ag40-Au5 for fixed incidence angles within 59°…70°. The vertical colored bars indicate the position of spectral components R (at 660 nm) and G (at 560 nm).

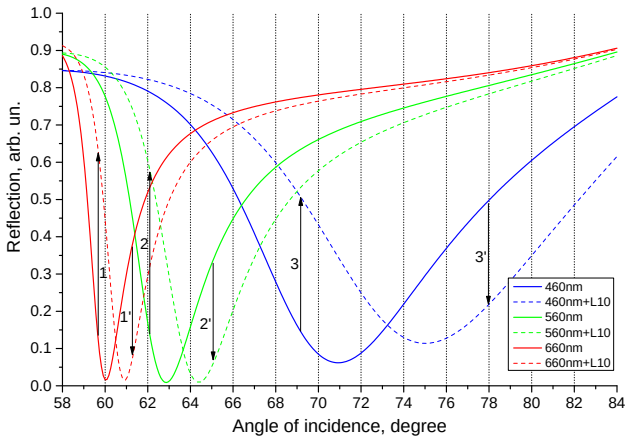

Fig. 5. The responses of internal reflection in a silver film to the appearance of a 10 nm thick dielectric layer with a refractive index of 1.48 at three incident light wavelengths corresponding to the R, G, B components: 660 nm (shown by arrows *1-1'*), 560 nm (*2-2'*), and 460 nm (*3-3'*).

optimal angle of incidence in this series of curves can be considered close to 63°, as the signal at the green wavelength increases with "adsorption", while at the red wavelength, it decreases. Thus, the advantage of RGB registration can be realized to enhance the response.

The reaction of the reflection coefficient R to the appearance of a thin dielectric film on the surface of the bimetallic layer for three wavelengths corresponding to the relevant red and green spectral regions for this case is demonstrated in Fig. 7. One can see that the obtained sensitivity is quite high. According to the criteria for the angular shift of SPR minimum and the change in the magnitude of the reflection, it lies within the following ranges, respectively: S_1 = 1°…2°, S_2 = 0.31…0.46 arb. un.

Thus, we can conclude that the option of bimetallic film is noticeably worse than that of a pure silver film because the spectral range of the existence of SPR within the short-wavelength range of the visible spectrum is significantly reduced.

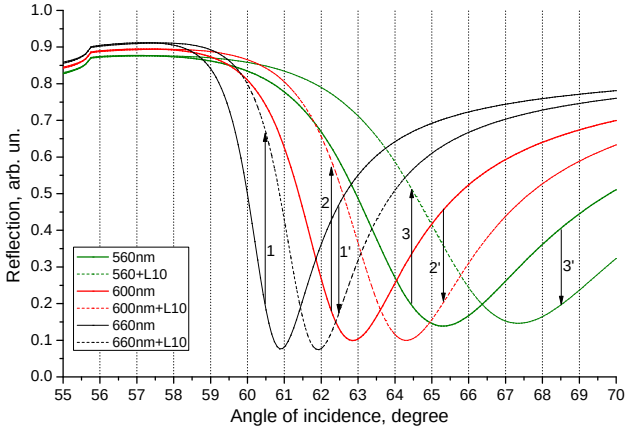

Fig. 7. The internal reflection responses in the Ag40-Au5 bimetallic structure to the appearance of a 10 nm thick dielectric layer with a refractive index of 1.48 at three incident light wavelengths: 660 nm (shown by arrows *1-1'*), 600 nm (*2-2'*), and 560 nm (*3-3'*).

Let us now consider other highly conductive metals as potential candidates for the principle of chromatic detection of adsorption using the registration of the R, G, and B components.

Copper

Figs. 8a and 8b show the angular dependences of internal reflection within the range of SPR excitation and the corresponding spectral dependences at different angles of light incidence, for a copper film of 35 nm thick. One can see that SPR is well excited only within the red range of the spectrum, as in the case of gold. As noted above, copper and gold have close optical constants within the visible range. However, compared to gold, copper still has a slightly larger real part of the permittivity within the short-wave region (see Fig. 1b). Nevertheless, this circumstance does not provide a noticeable advantage for copper, which is evident from the spectral characteristic of reflection (see Fig. 8b): within the green range of the spectrum, reflection is practically independent of the wavelength. Sharp signal fluctuations occur within the longer-wave red and near IR ranges. As a result, such characteristics do not allow the full use of copper for the realization of the chromatic mode of the SPR biosensor.

As follows from Fig. 8b, we can obtain a significant gain in sensitivity using the difference in signals at 660 nm (component R) in the mode of switching between two fixed angles of light incidence within 61°…62° and 65°…66°, since the responses at these angles have different signs.

Let us estimate the sensitivity of the reflection coefficient R for copper to the appearance of a thin dielectric film on the metal surface. This estimation for three wavelengths corresponding to the red range of the spectrum, relevant for copper, is demonstrated in Fig. 9. It is evident that the sensitivity is quite low. According to the above-introduced criteria S_1 and S_2, it varies within the limits, respectively: S_1 = 1°…1.6°, S_2 = 0.22…0.31 arb. un.

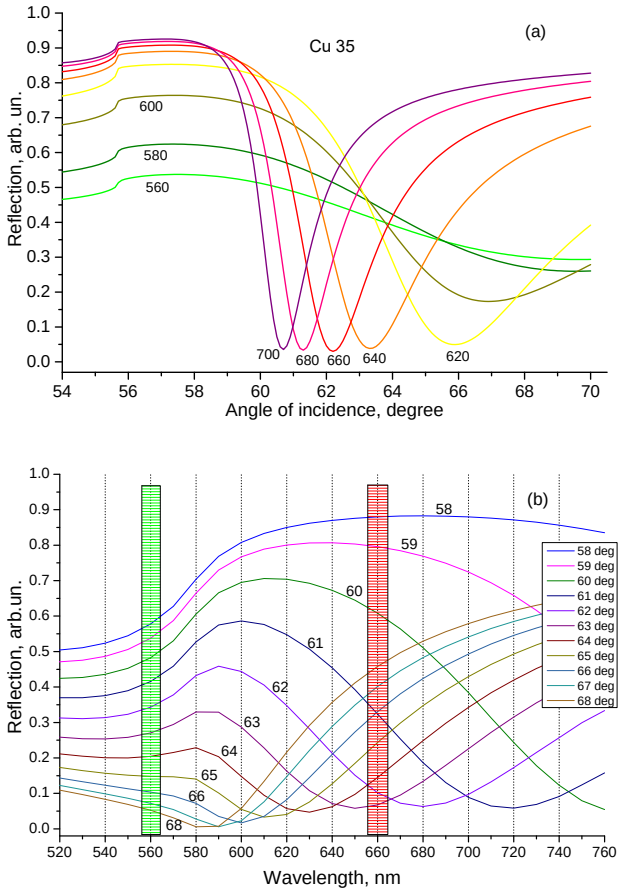

Fig. 8. The angular (a) and spectral (b) dependences of the reflection coefficient within the range of SPR excitation in a copper film of 35 nm thick.

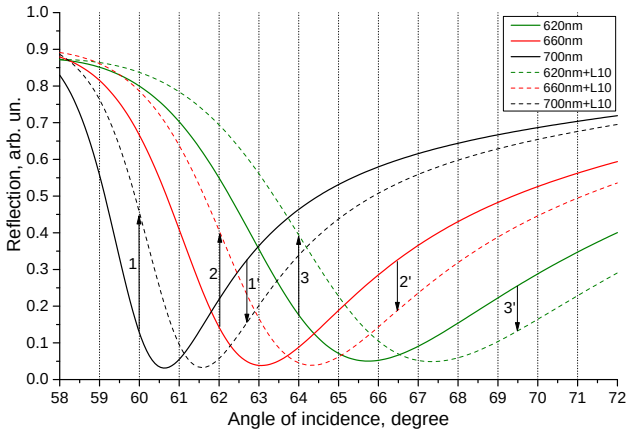

Fig. 9. The internal reflection responses in a 35 nm copper film to the appearance of a 10 nm thick dielectric layer with a refractive index of 1.48 at several incident light wavelengths: 700 nm (shown by arrows *1-1'*), 660 nm (*2-2'*), and 620 nm (*3-3'*).

Considering copper as a candidate for use in the chromatic SPR mode, we can summarize that copper films can fully operate only within the red range at wavelengths over 600 nm. Neither the green nor the blue ranges of the spectrum are accessible to them.

Aluminum

As follows from Fig. 1, aluminum is a very promising material for the SPR realization within the short-wavelength range of the visible spectrum, since the real part of its dielectric function ε_m is negative and significantly exceeds the corresponding values of other metals. Due to the high extinction coefficient k in aluminum, the electromagnetic wave attenuates very quickly, so in the Kretschmann geometry it is necessary to use very thin metal films. Fig. 10a shows the angular dependences of SPR for an aluminum film of 20 nm thick. As can be seen, the SPR curve has a pronounced narrow minimum within 57°…60° for the short-wavelength range of 400…560 nm. It is worth noting that the increasing part of the angular dependence very quickly reaches saturation and the maximum reflection does not exceed 0.6…0.7, unlike gold, copper, and silver films, where this value is 0.8…0.9. This is also a consequence of the high value of k.

However, the spectral dependences of reflection (see Fig. 10b) within 400…600 nm do not exhibit a pronounced U-shape. Only the curve at an incidence angle of 59° demonstrates some semblance of a minimum close to 430 nm. Thus, SPR is quite successfully realized only within the blue range of the spectrum.

By analogy with the other considered metals, let us estimate the sensitivity of reflection coefficient R to the

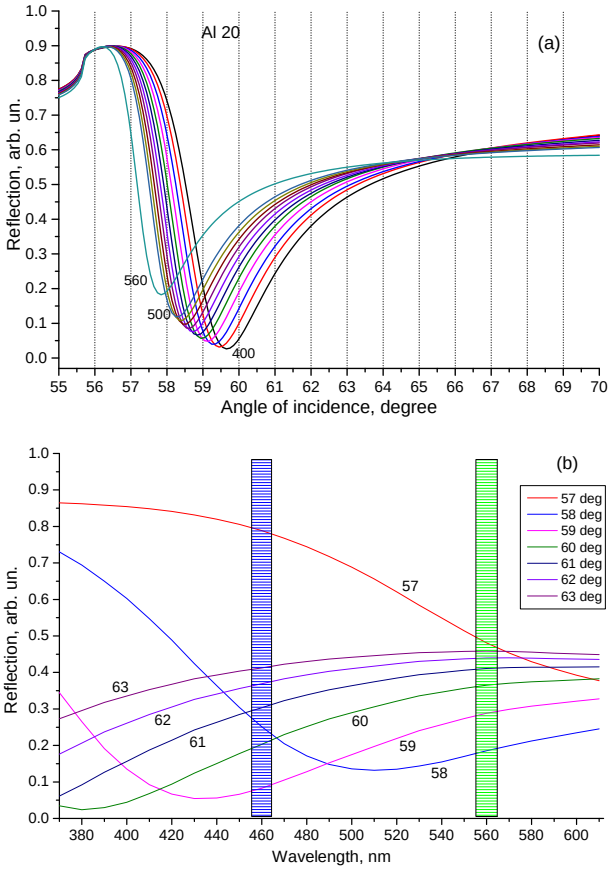

Fig. 10. The angular (a) and spectral (b) dependences of the reflection coefficient within the range of SPR excitation in an aluminum film of 20 nm thick.

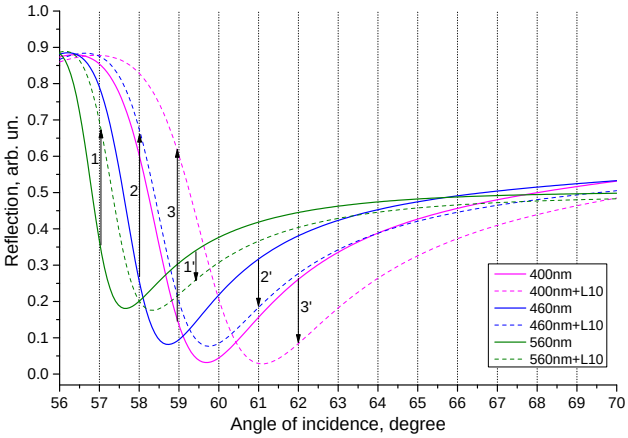

Fig. 11. The internal reflection responses in a 20 nm thick aluminum film to the appearance of a 10 nm thick dielectric layer with a refractive index of 1.48 at three incident light wavelengths: 560 nm (shown by arrows *1-1'*), 460 nm (*2-2'*), and 400 nm (*3-3'*).

appearance of a thin dielectric film on the aluminum surface. Fig. 11 demonstrates this estimation for three wavelengths corresponding to the blue part of the spectrum relevant just for aluminum. The obtained sensitivity is larger than the corresponding value for copper but less than for other considered metals. According to the above criteria S_1 and S_2, it lies within the limits, respectively: S_1 = 0.9°…1.5°, S_2 = 0.4…0.65 arb. un.

Thus, as follows from the above-obtained results, the excitation of a full-fledged SPR in an aluminum film is possible only within the blue range of the visible spectrum. Therefore, aluminum should also be excluded from the candidates for realizing a chromatic SPR sensor.

3. Results and discussion

Based on model calculations of the sensitivity of the SPR sensor to the appearance of a thin dielectric film on the metal surface (in fact, the sensitivity to the adsorption of the biomolecular layer), we carried out a quantitative analysis of the data obtained in the previous sections. In this case, the change in the reflection coefficient at a fixed angle of incidence for a given wavelength (the parameter S_2 introduced above) was taken as the main parameter. This parameter is important for the chromatic mode of the SPR. This quantitative data for all considered metals is presented in Table.

As can be seen from the provided data, silver has the highest sensitivity to the appearance of an external dielectric layer (simulating the adsorption layer of biomolecules), it has the largest changes in the value of the reflection coefficient at fixed angles of incidence within the entire visible range of the spectrum. This is obviously due to the presence of a resonance curve with steeper slopes compared to other metals.

The second (most sensitive) metal among the considered ones is the bimetallic structure of silver with a thin gold overlayer, and the third is pure gold. In general, the characteristics of these two variants are very close,

Table. The values of response to the appearance of a 10 nm thick dielectric layer with a refractive index of 1.48 for: (a) 50 nm thick gold film, (b) 40 nm silver, (c) bimetallic structure of 40 nm silver – 5 nm gold, (d) 35 nm copper, (i) 20 nm aluminum. The values of response are taken as the change in the reflection value at the indicated wavelengths.

(a)				
Au 50 Response, arb. un.	Wavelength, nm			Angle, degree
	600	660	720	
	0.23			65.5
	–0.14			73
Difference	**0.37**			
		0.36		62.5
		–0.23		66
Difference		**0.59**		
			0.46	61
			–0.29	63
Difference			**0.75**	

(b)				
Ag 40 Response, arb. un.	Wavelength, nm			Angle, degree
	460	560	660	
	0.36			69
	–0.27			78
Difference	**0.63**			
		0.44		62
		–0.26		65
Difference		**0.7**		
			0.5	59.5
			–0.3	61.3
Difference			**0.8**	

(c)				
Ag40-Au5 Response, arb. un.	Wavelength, nm			Angle, degree
	560	600	660	
	0.31			64.5
	–0.21			68.5
Difference	**0.52**			
		0.40		62.3
		–0.26		65
Difference		**0.66**		
			0.46	60.5
			–0.28	62.5
Difference			**0.74**	

(d)				
Cu 35 Response, arb. un.	Wavelength, nm			Angle, degree
	620	660	700	
	0.22			64
	–0.13			69.5
Difference	**0.35**			
		0.25		62
		–0.14		66.5
Difference		**0.39**		
			0.31	60
			–0.17	62.5
Difference			**0.48**	

(i)				
Al 20 Response, arb. un.	Wavelength, nm			Angle, degree
	400	460	560	
	0.48			59
	–0.17			62
Difference	**0.65**			
		0.4		58
		–0.13		61
Difference		**0.53**		
			0.32	57
			–0.08	59.5
Difference			**0.40**	

which is no coincidence, since it is the outer layer of the bimetallic structure near the metal-dielectric interface that essentially determines the conditions for generating plasmon-polaritons. Next in value of sensitivity is aluminum, which is significantly inferior to the previous options, but has a very effective blue region with good sensitivity within this range. Finally, copper has the lowest sensitivity among all considered metals.

To achieve higher sensitivity, we emphasize the possibility of using as a response not just a change in the value of reflection during adsorption of the biomolecular layer, but the difference in responses at various angles of light incidence, taking advantage of the opposite signs of the corresponding responses (see Table). In this way, it is possible to increase the value of response up to 1.5 times. Moreover, we can take into account the difference in the value of responses simultaneously for several different wavelengths close to R, G, and B components. This is realized especially effectively for silver films, where all three R, G, and B components work perfectly. Then the total difference response can reach more than 200 %. Note that a similar approach has already been experimentally tested by us in [43]. At the same time, for other metals, with a shortened range of SPR realization, such large responses as on silver cannot be achieved.

4. Approaches to the realization of a chromatic SPR biosensor

The proposed method of chromatic registration of molecular adsorption by monitoring the R, G, and B components of reflected light under conditions of plasmon-polariton resonance excitation can be realized when the lateral surface of a glass prism (with a refractive index greater than 1.61 for liquid media) is illuminated by a parallel collimated beam from a white light source. A thin layer of plasmon-active metal is applied to the base surface of the prism. Since in the previous sections we noted the advantages of silver in the realization of the chromatic mode, we will assume that a silver layer of 38…45 nm thick is used as a plasmonic metal, protected from above by a thin superlayer (units of nm) of chemically resistant polymer. The angle of incidence is selected within 50°…70° (relevant for liquid media). The reflected beam is directed to the video camera of the smartphone,

which can record and store the colored image of the illuminated surface in the *X* and *Y* coordinates.

A pattern of ligands that specifically react with analyte molecules (antibodies, DNA fragments, *etc*.) is applied to the silver surface. After the surface is brought into contact with the buffer solution, the initial distribution of RGB_0 (*X*, *Y*) values is recorded and stored. The liquid medium is then replaced with a sample containing a set of the studied molecules that have an affinity for the applied ligands and after the interaction of the analyte and ligand (receptor), a new distribution map of RGB_1 (*X*, *Y*) is recorded. To increase the sensitivity and reliability of molecule detection, it is advisable to record responses not only by changes in the color components ΔR, ΔG, and ΔB but also (considering the often opposite direction of the response) by changes in their differences ΔR–ΔG, ΔG–ΔB or ΔR–ΔB, which leads to at least a doubling of the difference signal.

5. Conclusions

It has been shown that the best option for realizing the SPR of biosensors in the chromatic mode is silver, it allows with equal success to obtain a full-fledged SPR effect within the widest visible range 400…700 nm. The calculations also have shown that silver is the best metal in terms of sensitivity to the appearance of an external dielectric layer (simulating the adsorption layer of biomolecules) by changing the value of the reflection coefficient at a fixed angle of incidence of the beam and shifting the angle of the SPR minimum at a fixed wavelength. For the first case, more important for assessing the chromatic SPR sensor, detailed quantitative characteristics were obtained for all the considered metals. Based on these characteristics, as well as the range of implementation of the full-fledged SPR effect, the considered metals can be arranged in descending order of quality as follows: silver – bimetal silver-gold – gold – aluminum – copper.

The second (most functional) variant is a bimetallic structure of silver with a thin gold overlayer. Although it is noticeably inferior to pure silver in the breadth of the SPR realization range, however, includes, in addition to the red, also a full green region of the spectrum. Another advantage of this structure is the chemical resistance of gold to oxidation. Third in this list is pure gold, which is only slightly inferior to the bimetallic structure. The other considered metals have a significantly lower potential, realizing SPR only within one specific range of the spectrum (copper – within the red, aluminum – within the blue), and thus cannot claim to implement a full-fledged chromatic SPR sensor.

The spectral analysis of the SPR effect using wide ranges of wavelengths and angles of light incidence also showed the possibility of successful operation of the sensor in a quasi-chromatic mode. In this case, for highly sensitive recording of responses, it is possible to use only a few selected wavelengths of the visible range at a fixed angle of incidence or several fixed angles at one wavelength. This approach can significantly simplify the design of a chromatic SPR sensor.

References

1. Homola J. Surface plasmon resonance sensors for detection of chemical and biological species. *Chem. Rev*. 2008. **108**. P. 462–493. https://doi.org/10.1021/cr068107d.
2. *Handbook of Surface Plasmon Resonance*, 2nd Ed., Ed. R. Schasfoort. The Royal Society of Chemistry, 2017. https://doi.org/10.1039/9781788010283-FP010.
3. Balbinot S., Srivastav A.M., Vidic J. *et al.* Plasmonic biosensors for food control. *Trends in Food Science & Technology*. 2021. **111**. P. 128–140. https://doi.org/10.1016/j.tifs.2021.02.057.
4. Hinman S.S., McKeating K.S., Cheng Q. Surface plasmon resonance: Material and interface design for universal accessibility. *Anal. Chem.* 2018. **90**, No 1. P. 19–39. https://doi.org/10.1021/acs.analchem.7b04251.
5. Ashley J., Piekarska M., Segers C. *et al.* An SPR based sensor for allergens detection. *Biosens. Bioelectron*. 2017. **88**. P. 109–113. https://doi.org/10.1016/j.bios.2016.07.101.
6. Rupert D.L.M., Shelke G.V., Emilsson G. *et al.* Dual-wavelength surface plasmon resonance for determining the size and concentration of sub-populations of extracellular vesicles. *Anal. Chem*. 2016. **88**, No 20. P. 9980–9988. https://doi.org/10.1021/acs.analchem.6b01860.
7. Sereda A., Moreau J., Boulade M. *et al.* Compact 5-LEDs illumination system for multi-spectral surface plasmon resonance sensing. *Sens. Actuators B*. 2015. **209**. P. 208–211. https://doi.org/10.1016/j.snb.2014.11.080.
8. Pilolli R., Visconti A., Monaci L. Rapid and label-free detection of egg allergen traces in wines by surface plasmon resonance biosensor. *Anal. Bioanal. Chem*. 2015. **407**, No 13. P. 3787–3797. https://doi.org/10.1007/s00216-015-8607-4.
9. Zeng Y.J., Wang L., Wu S.Y. *et al.* High-throughput imaging surface plasmon resonance biosensing based on an adaptive spectral-dip tracking scheme. *Opt. Express*. 2016. **24**. P. 28303–28311. https://doi.org/10.1364/OE.24.028303.
10. Pollet J., Janssen K.P.F., Knez K., Lammertyn J. Real-time monitoring of solid-phase PCR using fiber-optic SPR. *Small*. 2011. **7**, No. 8. P. 1003–1006. https://doi.org/10.1002/smll.201001984.
11. Wang R., Tombelli S., Minunni M. *et al.* Immobilisation of DNA probes for the development of SPR-based sensing. *Biosens. Bioelectron.* 2004. **20**. P. 967–974. https://doi.org/10.1016/j.bios.2004.06.013.
12. de Bruijn H.E., Kooyman R.P.H., Greve J. Choice of metal and wavelength for surface-plasmon resonance sensors: Some considerations. *Appl. Opt*. 1992. **31**, No 4. P. 440–442. https://doi.org/10.1364/AO.31.0440_1.
13. Manickam G., Gandhiraman R., Vijayaraghavan R.K. *et al.* Protection and functionalization of silver as an optical sensing platform for highly sensitive SPR based analysis. *Analyst*. 2012. **137**. P. 5265–5271. https://doi.org/10.1039/c2an35826c.

14. Zynio S.A., Samoylov A.V., Surovtseva E.R. *et al.* Bimetallic layers increase sensitivity of affinity sensors based on surface plasmon resonance. *Sensors*. 2002. **2**. P. 62–70. https://doi.org/10.3390/s20200062.
15. Karlsen S.R., Johnston KS., Jorgenson R.C., Yee S.S. Simultaneous determination of refractive index and absorbance spectra of chemical samples using surface plasmon resonance. *Sens. Actuators B*. 1995. **24-25**. P. 747–749. https://doi.org/10.1016/0925-4005(95)85165-8.
16. Nenninger G.G., Clendenning J.B., Furlong C.E., Yee S.S. Reference-compensated biosensing using a dual-channel surface plasmon resonance sensor system based on a planar lightpipe configuration. *Sens. Actuators B*. 1998. **51**. P. 38–45. https://doi.org/10.1016/S0925-4005(98)00218-4.
17. Mu Y., Zhang H., Zhao X. *et al.* An optical biosensor for monitoring antigen recognition. *Sensors*. 2001. **1**, No 3. P. 91–101. https://doi.org/10.3390/s10300091.
18. Malureanu R., Lavrinenko A. Ultra-thin films for plasmonics: a technology overview. *Nanotechnol. Rev*. 2015. **4**, No 3. P. 259–275. https://doi.org/10.1515/ntrev-2015-0021.
19. Dastmalchi B., Tassin P., Koschny T., Soukoulis C.M. A new perspective on materials for plasmonics. *Adv. Opt. Mater*. 2016. **4**. P. 177. https://doi.org/10.48550/arXiv.1604.07389.
20. Ansari G., Pal A., Srivastava A.K., Vermaet G. Detection of hemoglobin concentration in human blood samples using a zinc oxide nanowire and graphene layer heterostructure based refractive index biosensor. *Opt. Laser Technol*. 2023. **164**. P. 109495. https://doi.org/10.1016/j.optlastec.2023.109495.
21. Karki B., Trabelsi Y., Pal A. *et al.* Direct detection of dopamine using zinc oxide nanowire-based surface plasmon resonance sensor. *Opt. Mater*. 2024. **147**. P. 114555. https://doi.org/10.1016/j.optmat.2023.114555.
22. Singh T.I., Singh P., Karki B. Early detection of chikungunya virus utilizing the surface plasmon resonance comprising a silver-silicon-$PtSe_2$ multilayer structure. *Plasmonics*. 2023. **18**. P. 1173. https://doi.org/10.1007/s11468-023-01840-x.
23. Lin Z., Jiang L., Wu L. *et al.* Tuning and sensitivity enhancement of surface plasmon resonance biosensor with graphene covered Au-MoS_2-Au films. *IEEE Photon. J.* 2016. **8**, No 6. P. 1–8. https://doi.org/10.1109/jphot.2016.2631407.
24. Nguyen H.H., Park J., Kang S., Kim M. Surface plasmon resonance: A versatile technique for biosensor applications. *Sensors*. 2015. **15**, No 5. P. 10481–10510. https://doi.org/10.3390/s150510481.
25. Mostufa S., Akib T.B.A., Rana Md.M., Islam Md.R. Highly sensitive TiO_2/Au/graphene layer-based surface plasmon resonance biosensor for cancer detection. *Biosensors*. 2022. **12**, No 8. P. 603. https://doi.org/10.3390/bios12080603.
26. Shukla S., Grover N., Arora P. Resolution enhancement using a multi-layered aluminum-based plasmonic device for chikungunya virus detection. *Opt. Quantum Electron*. 2023. **55**, No. 3. https://doi.org/10.1007/s11082-022-04485-y.
27. Ouyang Q., Zeng S., Jiang L. Sensitivity enhancement of transition metal dichalcogenides/silicon nanostructure-based surface plasmon resonance biosensor. *Sci. Rep*. 2016. 6. P. 28190. https://doi.org/10.1038/srep28190.
28. Wu L., Guo J., Wang Q. *et al.* Sensitivity enhancement by using few-layer black phosphorus-graphene / TMDCs heterostructure in surface plasmon resonance biochemical sensor. *Sens. Actuators B*. 2017. **249**. P. 542–548. https://doi.org/10.1016/j.snb.2017.04.110.
29. Alam M.K., Dhasarathan V., Natesan A. *et al.* Human teeth disease detection using refractive index based surface plasmon resonance biosensor. *Coatings*. 2022. **12**, No 10. P. 1398. https://doi.org/10.3390/coatings12101398.
30. Wu L., You Q., Shan Y. *et al.* Few-layer $Ti_3C_2T_x$ MXene: A promising surface plasmon resonance biosensing material to enhance the sensitivity. *Sens. Actuators B*. 2018. **277**. P. 210–215. https://doi.org/10.1016/j.snb.2018.08.154.
31. Karki B., Vasudevan B., Uniyal A., Srivastava V. Hemoglobin detection in blood samples using a graphene-based surface plasmon resonance biosensor. *Optik*. 2022. **270**. P. 169947. https://doi.org/10.1016/j.ijleo.2022.169947.
32. Srivastava S., Singh S., Mishra A.C. *et al.* Surface plasmon resonance biosensor with high sensitivity for detecting SARS-CoV-2. *Plasmonics*. 2024. **8**. P. 1477–1488. https://doi.org/10.1007/s11468-024-02304-6.
33. Choodum A., Kanatharana P., Wongniramaikul W., NicDaeid N. Using the iPhone as a device for a rapid quantitative analysis of trinitrotoluene in soil. *Talanta*. 2013. **115**. P. 143–149. https://doi.org/10.1016/j.talanta.2013.04.037.
34. Kirchner E., Koeckhoven P., Sivakumar K. Predicting the performance of low-cost color instruments for color identification. *J. Opt. Soc. Am. A*. 2019. **36**, No 3. P. 368–376. https://doi.org/10.1364/JOSAA.36.000368.
35. Ellerbee A.K., Phillips S.T., Siegel A.C. *et al.* Quantifying colorimetric assays in paper-based microfluidic devices by measuring the transmission of light through paper. *Anal. Chem.* 2009. **81**, No 20. P. 8447–8452. https://doi.org/10.1021/ac901307q.
36. Cantrell K., Erenas M.M., de Orbe-Paya I., Capitan-Vallvey L.F. Use of the Hue parameter of the Hue, saturation, value color space as a quantitative analytical parameter for bitonal optical sensors. *Anal. Chem.* 2010. **82**. P. 531–542. https://doi.org/10.1021/ac901753c.
37. https://refractiveindex.info/ (accessed 05.08.2024)
38. Yang H.U., D'Archangel J., Sundheimer M.L. *et al.* Optical dielectric function of silver. *Phys. Rev. B.* 2015. **91**. P. 235137. https://doi.org/10.1103/PhysRevB.91.235137.
39. Babar S., Weaver J.H. Optical constants of Cu, Ag, and Au revisited. *Appl. Opt.* 2015. **54**. P. 477–481. https://doi.org/10.1364/AO.54.000477.

40. *Resonant Technologies GmbH*. http://www.restec.de (accessed 30.07.2024).
41. Zybin A., Grunwald C, Mirsky V.M. *et al*. Double-wavelength technique for surface plasmon resonance measurements: Basic concept and applications for single sensors and two-dimensional sensor arrays. *Anal. Chem*. 2005. **77**. P. 2393–2399. https://doi.org/10.1021/ac048156v.
42. Riabchenko O.V., Kukla O.L., Fedchenko O.N. *et al.* SPR chromatic sensor with colorimetric registration for detection of gas molecules. *SPQEO*. 2023. **26**. P. 343–351. https://doi.org/10.15407/spqeo26.03.343.
43. Fedchenko O.N., Riabchenko O.V., Kukla O.L., Shirshov Yu.M. Gas sensor based on the spectral SPR effect with colorimetric registration of responses. *Sensor Electronics and Microsystem Technologies*. 2023. **20**, No. 3. P. 38–50. https://doi.org/10.18524/1815-7459.2023.3.288158.

Authors and CV

O.L. Kukla, Doctor of Sciences in Physics of Devices, Elements and Systems at the V. Lashkaryov Institute of Semiconductor Physics, Head of the Department of Chemobiosensorics. His area of scientific activity include the development and design of chemical, biological sensors, sensor arrays for biotechnology, medicine and ecology, study of molecular adsorption effects in polymer, biopolymer and composite thin layers. E-mail: alex.le.kukla@gmail.com, https://orcid.org/0000-0003-0261-982X

Yu.M. Shirshov, Doctor of Sciences in Physics and Mathematics (1991), Professor – scientific consultant at the V. Lashkaryov Institute of Semiconductor Physics. The area of his scientific interests includes molecular phenomena on semiconductor and insulator surfaces, optoelectronic and microelectronic chemical sensors and biosensors. E-mail: y_shirshov@hotmail.com

A.I. Biletskiy graduated from the T. Shevchenko Kyiv National University with M.S. degree in applied physics. PhD student at the V. Lashkaryov Institute of Semiconductor Physics (2023), and engineer (2024). His professional activities include the development of optical measuring setup based on surface plasmon resonance, the study of spectroscopy of radiation from plasmon-photon scattering in thin films of high conducting materials. https://orcid.org/0009-0007-2074-3839, e-mail: belanton11@gmail.com

O.N. Fedchenko graduated from Lviv Polytechnical Institute in 1964 with M.S. degree in semiconductors devices. Since 2010 he is with the V. Lashkaryov Institute of Semiconductor Physics as researcher. His scientific interests include the study of thin-film chemical gas sensors color RGB-spectroscopy and the development of optoelectronic colorimetric analyzers. E-mail: fedchenkoaleksandr50@gmail.com

Authors' contributions

Kukla O.L.: project administration, methodology, formal analysis, writing – original draft, visualization.

Shirshov Yu.M.: conceptualization, formal analysis, writing – original draft.

Biletskiy A.I.: methodology, formal analysis, data curation, visualization.

Fedchenko O.N.: investigation, validation, resources.

Спектральний ефект ППР у тонких плівках високопровідних металів та особливості реалізації ППР-біосенсорів у хроматичному режимі

О.Л. Кукла, Ю.М. Ширшов, А.І. Білецький, О.М. Федченко

Анотація. У роботі проведено оцінку застосування різних типів високопровідних металів для реалізації спектрального ефекту ППР (поверхневий плазмонний резонанс) у видимій області спектра для досягнення більш ефективної та продуктивної реєстрації біомолекул у рідкому середовищі із застосуванням триколорних RGB-камер. Розглянуто тонкі плівки золота, срібла, міді та алюмінію, а також біметалічного покриття срібла із надшаром золота на скляній підкладці. Проведено детальні розрахунки спектральних характеристик відбиття при збудженні ППР у геометрії Кретчмана, зокрема при утворенні на поверхні металу тонкої діелектричної плівки, що імітує шар біомолекул. Для кожного із зазначених металів визначено ширину області реалізації повноцінного ефекту ППР у видимому діапазоні спектра, а також проведено оцінку чутливості оптичного відгуку до впливу зовнішнього діелектричного шару.

Ключові слова: спектральний ефект ППР, хроматичний режим, високопровідні метали, спектри відбиття, R, G, B компоненти, видимий діапазон спектра.